Brian H. Dennis
Research Associate
Frontier Simulation Software for Industrial
Science Collaborative Research Center
Institute of Industrial Science
University of Tokyo
4-6-1 Komaba, Muguro-ku, Tokyo 153-8505,
Japan

Robert C. Eberhart
Professor of Engineering in Surgery
Department of Surgery and Biomedical
Engineering Program
The University of Texas Southwestern Medical
Center at Dallas
5323 Harry Hines Blvd. Dallas, TX 75390-9130

George S. Dulikravich
Professor, Director of MAIDO Institute
Department of Mechanical and Aerospace
Engineering, MAIDO Institute
The University of Texas at Arlington,
UTA Box 19018, Arlington, TX 76019

Steve W. Radons
Manager
Research & Development, Medtronic
Physio-Control Corporation
11811 Willows Road NE, P.O. Box 97006,
Redmond, WA 98073-9706

Finite-Element Simulation of Cooling of Realistic 3-D Human Head and Neck

Rapid cooling of the brain in the first minutes following the onset of cerebral ischemia is a potentially attractive preservation method. This computer modeling study was undertaken to examine brain-cooling profiles in response to various external cooling methods and protocols, in order to guide the development of cooling devices suitable for deployment on emergency medical vehicles. The criterion of successful cooling is taken to be the attainment of a 33°C average brain temperature within 30 min of treatment. The transient cooling of an anatomically correct realistic 3-D head and neck with realistically varying local tissue properties was numerically simulated using the finite-element method (FEM). The simulations performed in this study consider ice packs applied to head and neck as well as using a head-cooling helmet. However, it was found that neither of these cooling approaches satisfies the 33°C temperature within 30 min. This central conclusion of insubstantial cooling is supported by the modest enhancements reported in experimental investigations of externally applied cooling. The key problem is overcoming the protective effect of warm blood perfusion, which reaches the brain via the uncooled carotid arterial supply and effectively blocks the external cooling wave from advancing to the core of the brain. The results show that substantial cooling could be achieved in conjunction with neck cooling if the blood speed in the carotid artery is reduced from normal by a factor of 10. The results suggest that additional cooling means should be explored, such as cooling of other pertinent parts of the human anatomy. [DOI: 10.1115/1.1634991]

I. Introduction

Rapid cooling of the brain in the first minutes following the onset of cerebral ischemia is a potentially attractive preservation method. This computer modeling study was undertaken to examine brain-cooling profiles in response to various external cooling methods and protocols, in order to guide the development of emergency vehicle portable cooling devices. The devices considered in this research are noninvasive and would be applied to the external surface of patient's head and neck. Specifically, this study considers ice packs applied to the head and neck as well as a head-cooling helmet. The overall goal is to guide the development of these devices to obtain a 33°C average target temperature in the brain within 30 min of treatment [1] so that the procedure could be applied by medical emergency vehicle teams. Cooling the brain to a lower temperature would increase the risk of uncontrolled shivering and cardiac arrest.

Clinical devices and processes for brain cooling, and analytical methods for predicting temperature distributions have been reviewed [2]. The reason for cooling the brain is justified by a well-known "Q_{10} law" of thermal physiology. This law states that for every 10°C reduction in tissue temperature there is a corresponding reduction in brain cell metabolism equal to the constant Q_{10}. Values for Q_{10} range from 2.0 to 3.0 and are cited in the physiology literature. The law is written as:

$$\frac{q_m}{q_{m0}} = Q_{10}^{[(\theta-\theta_0)/10]} \tag{1}$$

where θ is temperature and q_m is the cell metabolic rate. Assuming a mid-range value, say $Q_{10}=2.5$, it is seen that reducing tissue temperature from 37°C to 34°C reduces the metabolic rate by about 25%. These values underscore the promise of cooling for cerebral protection.

During the past few years, several researchers have made attempts at numerically modeling cooling of oversimplified geometries of a human head while using equally oversimplified approaches to accounting for the actual diverse tissues in the head [2]. Our group has previously applied a less sophisticated finite-element method (FEM) to simulate transient brain cooling in a reasonably simplified 2-D cylindrical geometric model of a subhuman primate, the macaque rhesus monkey [3–5]. Cooling was driven either by ice packs applied to the scalp, or by direct exchange with arterial blood via the heat exchanger in a heart-lung machine, or by both means. While the computational grid was less intricately prepared than in the current work, the predictions of that cooling simulation agreed reasonably well with direct experimental measurements at multiple sites within the brain.

The main benefit of the research effort presented here is that it uses a realistic fully 3-D geometry of an actual human head and realistic values for thermo-physical properties of a large number of local tissues constituting the head. The numerical algorithm is also highly accurate and computationally efficient. The results will offer significantly more definitive answers as to the feasibility of brain cooling via non-intrusive means.

II. Finite-Element Model (FEM)

An approximate temperature distribution throughout a perfused tissue can be found by solving bioheat transfer equation suggested by Pennes [6]:

$$\rho C_p \frac{\partial \theta}{\partial t} = \nabla \cdot (k \nabla \theta) + M_b C_p (\theta_{art} - \theta) + q_m \tag{2}$$

Here, θ_{art} is the arterial perfusion temperature and q_m is the heat source due to metabolism. The perfusion term is $M_b C_p(\theta_{art}$

Contributed by the Bioengineering Division for publication in the JOURNAL OF BIOMECHANICAL ENGINEERING. Manuscript received by the Bioengineering Division June 17, 2002; revision received July 25, 2003. Associate Editor: E. P. Scott.

$-\theta$), where M_b is the capillary perfusion rate, measured in ml blood flow per minute per ml of tissue. This "rate" can be understood as blood flow through the millions of capillaries in the tissue, proceeding in all directions at once, and thus not having a vector form. Additionally, we assume temperature-independent material properties and heat source terms. Under these conditions, analytic solutions can be found only for very simple geometries. For realistic configurations, we must resort to numerical approximations of the bioheat transfer equation. A FEM, which is described here, was used [7]. In the FEM, the domain where the solution is sought is divided into a finite number of parts called elements. In this work, tetrahedral shaped elements were used exclusively since almost any complex 3-D geometry, including a human head, can be decomposed into a finite number of well-shaped tetrahedral elements.

Applying the method of weighted residuals to Eq. (2) over a single tetrahedral element Ω^e with weight function v results in:

$$\int_{\Omega^e} v\left\{\rho C_p\frac{\partial\theta}{\partial t}-k\left(\frac{\partial^2\theta}{\partial x^2}+\frac{\partial^2\theta}{\partial y^2}+\frac{\partial^2\theta}{\partial z^2}\right)-M_bC_p(\theta_{art}-\theta)-q_m\right\}d\Omega^e=0 \tag{3}$$

Integrating Eq. (3) by parts once creates the weak statement for the element:

$$\int_{\Omega^e} v\rho C_p\frac{\partial\theta}{\partial t}d\Omega^e+\int_{\Omega^e}k\left(\frac{\partial v}{\partial x}\frac{\partial\theta}{\partial x}+\frac{\partial v}{\partial y}\frac{\partial\theta}{\partial y}+\frac{\partial v}{\partial z}\frac{\partial\theta}{\partial z}\right)+vM_bC_p\theta d\Omega^e=\int_{\Omega^e}v(M_bC_p\theta_{art}+q_m)d\Omega^e-\int_{\Gamma^e}v(\vec{q}\cdot\vec{n})d\Gamma^e \tag{4}$$

Here, Γ^e is the element of the surface. Variation of the temperature across the element can be expressed by:

$$\theta(x,y,z)=\sum_{i=1}^{m}N_i(x,y,z)\,\theta_i \tag{5}$$

Here, i is an element local node number, m is the total number of element nodes, and N is the shape function associated with node i. Using Galerkin's method, the weight function v and the interpolation function for θ are chosen to be the same. By defining the matrix $[B]$ as:

$$[B]=\begin{bmatrix}\frac{\partial N_1}{\partial x} & \frac{\partial N_2}{\partial x} & \cdots & \frac{\partial N_m}{\partial x}\\ \frac{\partial N_1}{\partial y} & \frac{\partial N_2}{\partial y} & \cdots & \frac{\partial N_m}{\partial y}\\ \frac{\partial N_1}{\partial z} & \frac{\partial N_2}{\partial z} & \cdots & \frac{\partial N_m}{\partial z}\end{bmatrix} \tag{6}$$

the weak statement in Eq. (4) can be written in the matrix form as:

$$[\mathrm{C^e}]\left\{\frac{\partial\theta^{\mathrm{e}}}{\partial \mathrm{t}}\right\}+[\mathrm{K_c^e}]\{\theta^{\mathrm{e}}\}=\{\mathrm{R^e}\} \tag{7}$$

The local stiffness matrix, $[K_c^e]$, the local capacitance matrix, $[C^e]$, and the right-hand side vector, $\{R^e\}$, are evaluated as:

$$[K_c^e]=\int_{\Omega^e}k[B]^T[B]+M_bC_p\{N\}\lfloor N\rfloor d\Omega_e \tag{8}$$

$$[C^e]=\int_{\Omega^e}\rho C_p\{N\}\lfloor N\rfloor d\Omega_e \tag{9}$$

$$\{R^e\}=\int_{\Omega^e}(q_m+M_bC_p\theta_{art})\{N\}d\Omega_e-\int_{\Gamma^e}q_s\{N\}d\Gamma^e \tag{10}$$

for each element in the domain and then assembled into the global system of linear ordinary differential equations:

$$[C]\{\dot{\theta}\}+[K_c]\{\theta\}=\{R\} \tag{11}$$

This global system of equations can be solved to obtain the approximate solution to the bioheat transfer equation of the entire domain. Here, the time derivative of temperature, $\{\dot{\theta}\}$, is discretized using a finite difference approximation in time. The Crank-Nicolson algorithm is used and the final linear system of algebraic equations can be written as

$$\left(\frac{1}{2}[K_c]+\frac{1}{\Delta t}[C]\right)\{\theta_{n+1}\}=\left(-\frac{1}{2}[K_c]+\frac{1}{\Delta t}[C]\right)\{\theta_n\}+\frac{1}{2}(\{R\}_{n+1}+\{R\}_n) \tag{12}$$

where the subscript $n+1$ denotes the current time step and n denotes previous time step.

The approximate solution approaches the exact solution as the number of elements is increased and as the time step size, Δt, is reduced. However, increasing the number of elements and increasing the number of time steps also increases the computational cost. Therefore, the analyst must choose a computational grid and time step size that will give acceptable results in a reasonable amount of computational time.

The FEM was implemented in a C++ code. The code was written to be computationally efficient so that realistic simulations can be performed on a typical personal computer. The linear algebraic system is solved at each time step using an iterative sparse matrix solver based on conjugate gradient method with an incomplete factorization for preconditioning [8]. The solution for the previous time step is used as the initial guess for the iterative solver on the next time step, which provides enhanced convergence rates. A typical time-accurate numerical simulation can be performed on a notebook PC (PIII 700 MHz) in less than 20 min using less than 64 MB of in-core memory [9–11]. The FEM and the computer code used in the present work were verified with a geometrically simple problem for which a closed-form solution is available: excellent agreement was obtained [9,10]. Therefore, we have full confidence in the accuracy of the current FEM results.

In order to perform a finite-element simulation, a geometrical object must first be defined and discretized into a computational grid made of tetrahedral elements. The head geometry used in this research was constructed from the National Library of Medicine's Standard Man data [12], which was derived from 1 mm thick sections of an entire male cadaver. A 3-D tetrahedral grid of the head was generated from these data by researchers at the University of Karlsruhe [13,14]. It was composed of 43448 linear tetrahedrons with 14 material property domains, including air cavities within the head. The triangular surface grid is shown in Fig. 1. The underlying voxel representation we used is the result of the tissue classification of the Visible Man Dataset by the Karlsruhe University team [13,14]. Capillary "tissue" perfusion data from an experimental study of rapid brain cooling in a subhuman primate model at the University of Texas Southwestern Medical Center at Dallas [15,16] was adapted to human tissue types.

Consensus values of thermal parameters for various body tissues were used, as given in Table 1 [15–18]. The steady state and transient Pennes equations were discretized among all computational nodes and solved for various initial, boundary and perfusion conditions.

In addition, an idealized neck problem was formulated in order to concentrate on the convective heat transfer contributions of the carotid artery and internal jugular vein, the primary conduits for transfer of heat to and from the brain from an ice bath surrounding the neck. This "countercurrent heat exchanger" problem was formulated for a geometry based on an idealized neck anatomy derived from the website www.vesalius.com rather than from the discrete NLM/Karlsruhe data. This was done in part to simplify

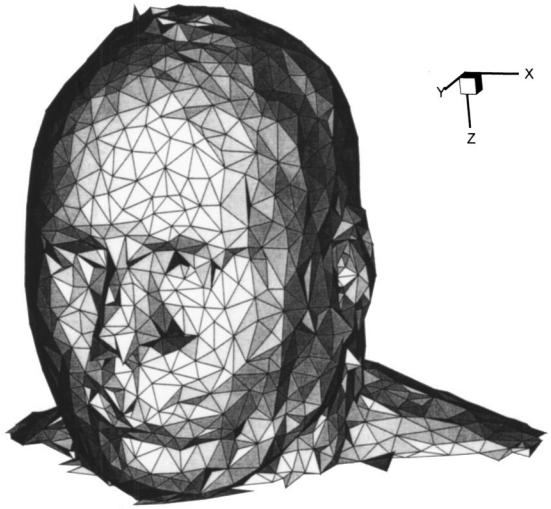

Fig. 1 View of the triangular surface mesh of the realistic human head [13,14]

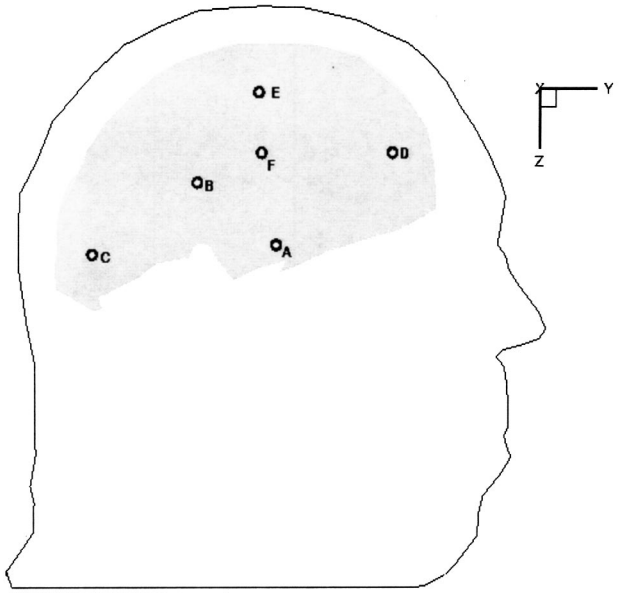

Fig. 2 Temperature monitor points on a vertical symmetry slice taken in the middle of head

the problem and in part to adjust the anatomy of the overdeveloped neck of the cadaver source of the NLM data. Thus, a separate 3-D computational grid was generated for this idealized geometry of the neck in order to emphasize temperature gradients in the vicinity of the carotid artery and internal jugular vein, which are relatively close to the neck surface. The head and neck computational grid, thermal and perfusion parameters and numerical results are available in animation, graphical, and tabular form at http://maido.uta.edu/~brian/research/head/head.html.

III. Numerical Results for Head Cooling

Head Cooling With Ice Surface Temperature. In the FEM simulation of cooling of a realistic 3-D human head, only the face, eyes and nose were assumed to be at the steady room temperature of 25°C. The base of the head was at a steady temperature of 37°C. In all cases, the temperature was monitored at six points within the brain. The locations of the monitor points are shown in Fig. 2. The simulation was terminated when all six points reached the target temperature of 33°C.

The following four test cases were numerically analyzed:

Case 1. No tissue perfusion and $\theta_{surf}=0°C$ at t=0 for the regions covered by a garment maintained at ice temperature.

Case 2. Tissue perfusion at internal elements, using reasonable values adapted from the UT Southwestern rhesus monkey experimental hypothermia series [3,4]. The same surface element boundary conditions as in Case 1 and $\theta_{art}=35°C$.

Case 3. A repeat of Case 2 with $\theta_{art}=33°C$.

Case 4. A repeat of Case 2 with $\theta_{art}=31°C$.

Case 1. Surface at Ice Temperature, No Perfusion Cooling As shown in Fig. 3, without perfusion cooling of the brain, all tissues within the skull cool very slowly. Brain temperatures do not reach the 33°C target within 30 min of the onset of surface cooling (Fig. 4), although the brain did reach this target in 70 min (Fig. 5). This result suggests that surface-only cooling at $\theta_{surf}=0.0°C$ would not be a viable method for protection of the brain following the onset of cerebral ischemia.

For possible applications in mobile emergency units, it is of interest to know the energy requirements for performing the cooling of a brain. The total energy removed via the skin at 70 min in this test case was 386 kJ requiring a total average power of 92 watts (Fig. 6). The predicted peak power (as estimated by back-

Table 1 Physical properties of tissues used in thermal modeling of a human head and neck

Tissue Type	Conductivity (k) ($W\,m^{-1}\,°C^{-1}$)	Specific Heat (C_p) ($J\,kg^{-1}\,°C^{-1}$)	ρC_p ($J\,m^{-3}\,°C^{-1}$)*10^6	Perfusion (M_b) ($kg\,m^{-1}\,s^{-1}$)	Metabolic Rate (q_m) ($W\,m^{-3}$)
Skin	0.34	2495.0	3.7	0.433	33.0
Fat	0.21	2495.0	3.7	0.3	33.0
Muscle	0.52	3543.0	3.7	0.433	33.0
Bone	1.16	1500.0	2.4	0.066	5.0
Brain matter	0.52	3680.0	3.7	8.6	525.0
Eye	0.52	···	3.7	0	0
Liquor	0.52	···	3.7	0	0
Lens	0.34	···	3.7	0	0
Neural tissue	0.52	···	3.7	0	0
Optic nerve	0.52	···	3.7	0	0
Cartilage	0.52	···	3.7	0	0
Mucous membrane	0.0252	···	0.991	0	0
Glands	0.52	···	3.7	0	0
Air	0.0252	···	0.991	0	0
Blood	0.5		4.3	0	0

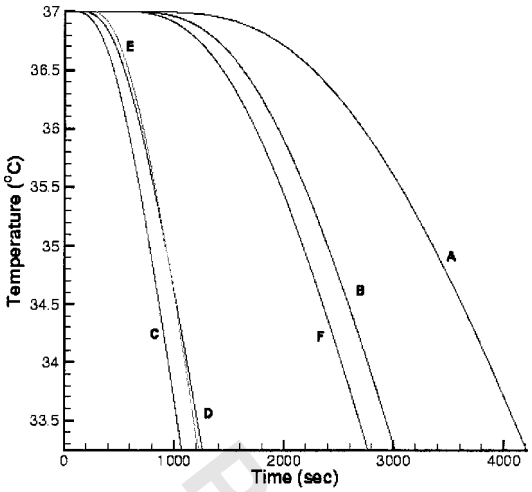

Fig. 3 Temperature evolution at monitor points in the brain for Case 1 (no tissue perfusion and θ_{surf}=0°C)

ward extrapolation close to t=0) was over 200 watts. The absolute peak power value (at t=0) was not calculated, since this modeling method requires extremely small grid sizes and time increments near the surface and at t=0, and unduly burdens the model. Furthermore, the instantaneous power level at the sudden onset of θ_{surf}=0°C is unrealistic since in reality a θ_{surf}=0°C boundary condition at the skin would be established over a short period of time (seconds). Currently, it would not be possible to simulate that temporal change in the surface boundary condition without also modeling the ice-water phase change, that is, the latent heat effects at the surface of the head.

Case 2. Surface at Ice Temperature, Perfusion Cooling With $\theta_{art}=35°C$. In this case the brain still does not reach the 33°C target within 30 min of combined cooling. In fact, a significant portion of the brain does not reach 34°C within 30 min (Fig. 7). The reason for this is that the θ_{art}=35°C counteracts the conduction-based cooling from the surface. The predicted total energy removed from the skin surface was 1700 kJ (Fig. 7), which is irrelevant, since the 33°C was not reached.

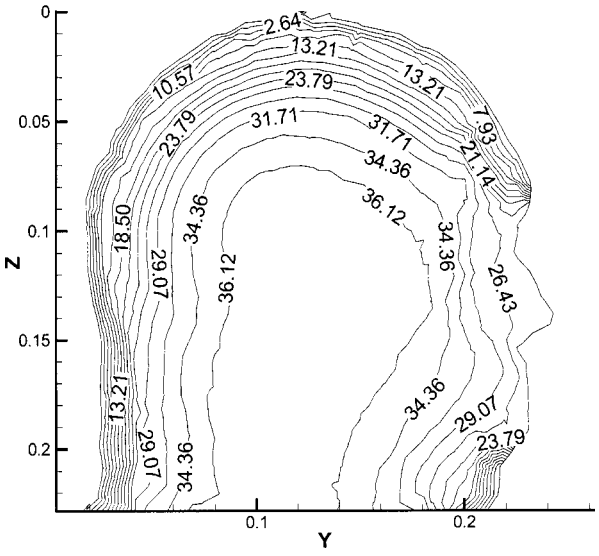

Fig. 4 Temperature contours on slice through middle of head for Case 1 (no tissue perfusion and θ_{surf}=0°C) after 30 min of cooling

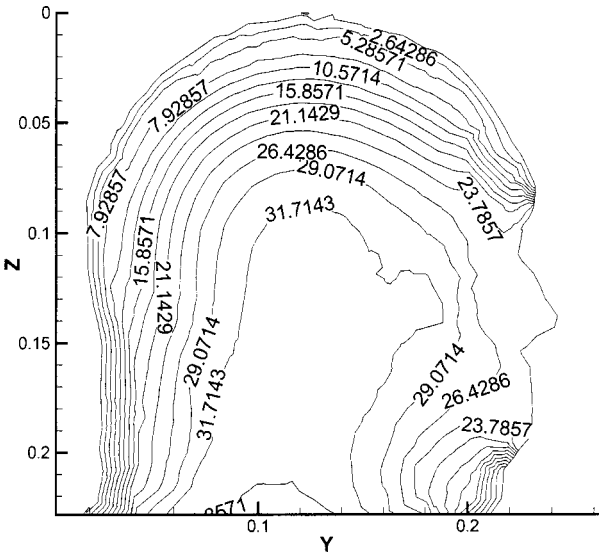

Fig. 5 Temperature contours on slice through middle of head for Case 1 (no tissue perfusion and θ_{surf}=0°C) after 70 min of cooling

Case 3. Surface at Ice Temperature, Perfusion Cooling With $\theta_{art}=33°C$. With entering arterial blood cooled at θ_{art}=33°C the brain reaches the 33°C target after approximately 7.5 min (Figs. 8, 9 and 10). It was predicted that a total of 94.7 kJ needs to be removed at an average rate of 210 watts and a near-initial peak power of 250 watts (Fig. 8). This means that less total energy needs to be removed than in Case 1, but the average and peak powers are higher, due to the additional cooling load of the incoming blood to the brain.

Case 4. Surface at Ice Temperature, Perfusion Cooling With $\theta_{art}=31°C$. With blood pre-cooled at θ_{art}=31°C the brain reaches the 33°C target at approximately two min (Fig. 11). A total of 44.8 kJ had to be removed at an average power of 344 watts and a near initial peak power of 250 watts (Fig. 11).

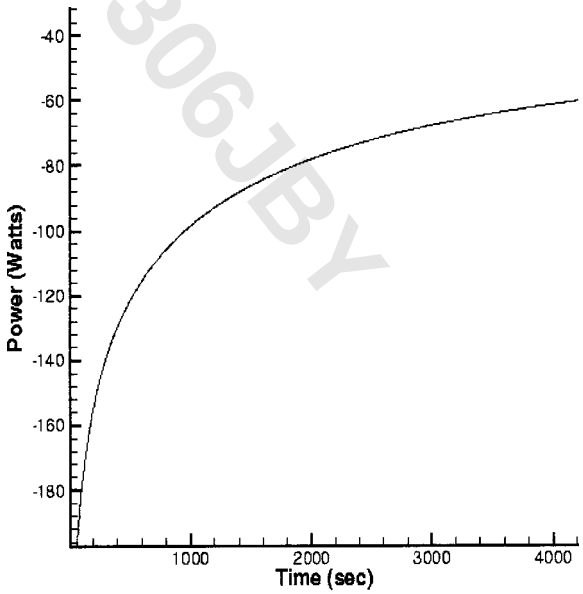

Fig. 6 Power transferred across surface of the head for Case 1 (no tissue perfusion and θ_{surf}=0°C)

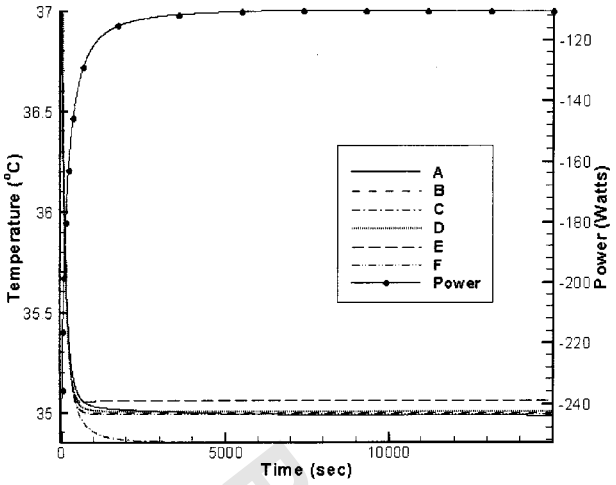

Fig. 7 Temperature evolution at monitor points in the brain and power transferred across surface of the head for Case 2 (tissue perfusion with $\theta_{surf}=0°C$ and $\theta_{art}=35°C$)

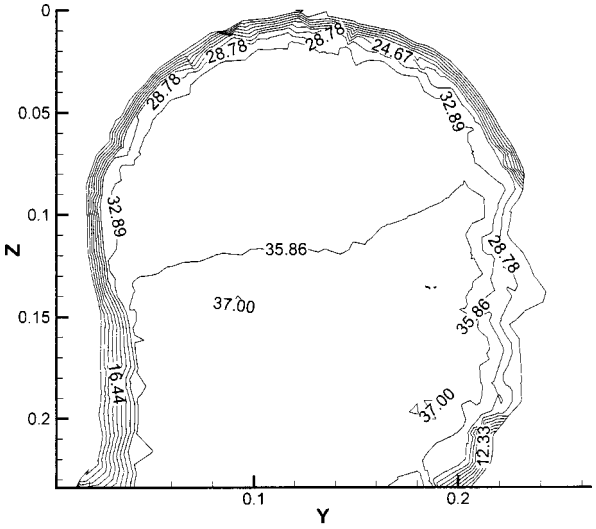

Fig. 9 Temperature contours on a slice through middle of the head for Case 3 (tissue perfusion with $\theta_{surf}=0°C$ and $\theta_{art}=33°C$) after 4 min of cooling

It is important to remember in Cases 2, 3 and 4 that the energy load associated with cooling the arterial blood to the specified temperatures was not included. Assuming the arterial blood enters the head/neck region at the normal temperature of $\theta_{art}=37°C$, with an arterial blood flow rate of 250 ml/min (which is less than normal), the additional average power load for 60 min of neck cooling would be 20 watts.

Cases 1–4 suggest that brain cooling to the target level of 33°C within 30 min is feasible *if* the arterial supply can be accessed and the arterial temperature reduced to these levels (at least $\theta_{art}=33°C$). Thus, efforts should be made to cool the arterial blood, examining all possible modalities. By inference, these results suggest that the brain may cool to the target level in time, if the head surface temperature $\theta_{surf}=-15°C$ is applied.

The perfusion-assisted results of Cases 2–4 agree in general with the experimental results of the UT Southwestern study of primates [3,4] and underscore the importance of the blood-based convective mechanism in tissue cooling. The midline temperature profiles in the animations of Cases 3 and 4 indicate more rapid cooling of the cortical and subcortical regions than deeper structures. This is expected, since the conduction pathway is shorter to these regions than to the deeper structures, and there is some lateral conduction owing to the curvature of the skull. A principal assumption of this analysis is that the perfusion distribution is uniform for all brain substructures, albeit significantly higher than for non-cerebral structures.

Of course, the patient with a cerebral ischemic event would not benefit from perfusion-cooling of the region of ischemia. This would imply that convective cooling would not be available, and that the region most in need of the protection of lower temperature would not receive it. However, brain perfusion distribution is quite volatile in healthy subjects, with blood flow rapidly shifting to regions experiencing high metabolism, as elegantly demonstrated by functional SPECT and MRI studies. This raises the important question of the regulation of blood supply to regions adjacent to the ischemic region: how, if at all, is the perfusion of these regions affected? Speculating for the moment that perfusion is unaltered in the adjacent regions; one may envision a potentially dangerous region of warm ischemia, surrounded by better-perfused, cooler tissues. In contrast to the results of cerebral hy-

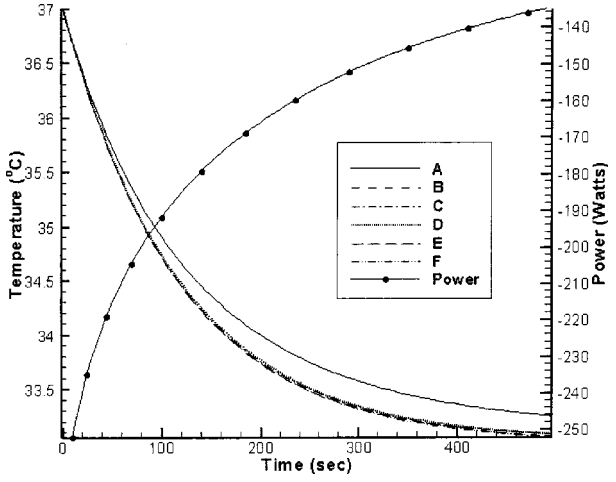

Fig. 8 Temperature evolution at monitor points in the brain and power transferred across surface of the head for Case 3 (tissue perfusion with $\theta_{surf}=0°C$ and $\theta_{art}=33°C$)

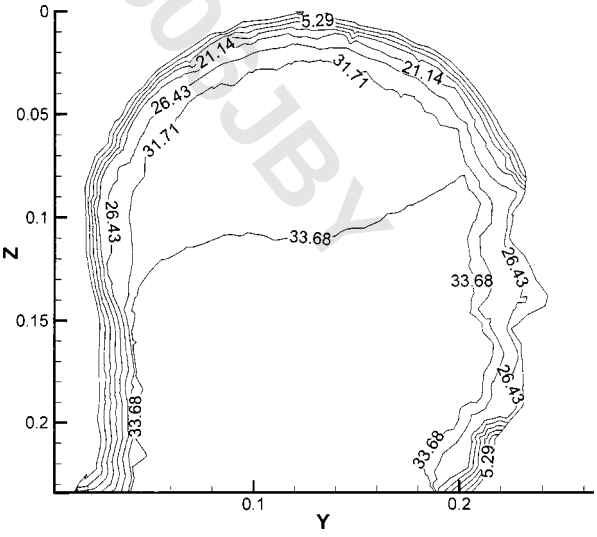

Fig. 10 Temperature contours on a slice through middle of the head for Case 3 (tissue perfusion with $\theta_{surf}=0°C$ and $\theta_{art}=33°C$) after 8 min of cooling

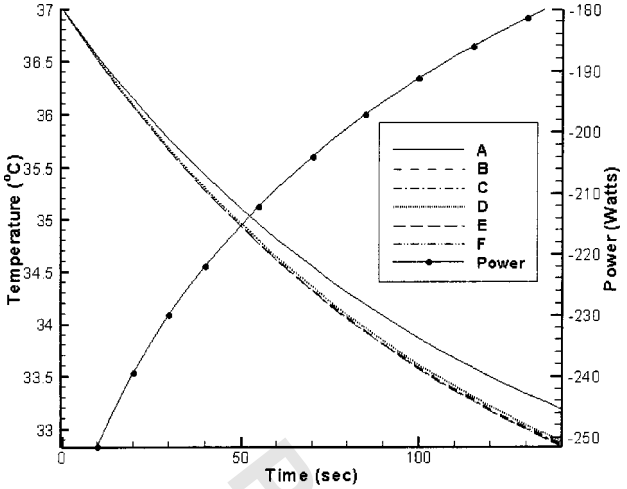

Fig. 11 Temperature evolution at monitor points in the brain and power transferred across surface of the head for Case 4 (tissue perfusion with $\theta_{surf}=0°C$ and $\theta_{art}=31°C$)

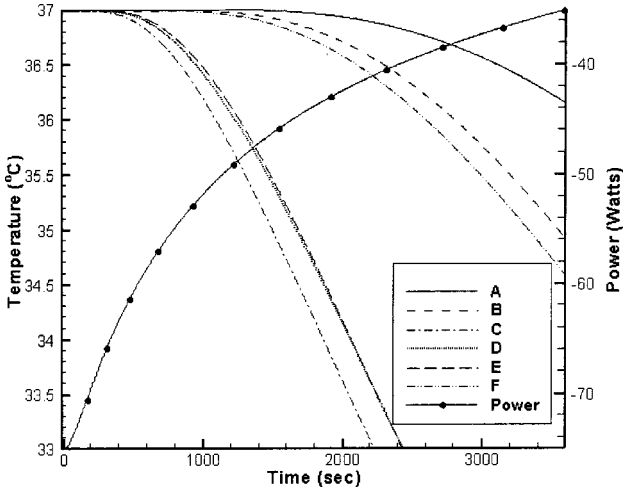

Fig. 12 Temperature evolution at monitor points in the brain and power transferred across surface of the head for Case 5 with cooled helmet (no tissue perfusion with $\theta_{surf}=0°C$ and surface heat transfer coefficient $h_{surf}=25.0\ W\,m^{-2}\,°C^{-1}$)

poxia modeling, thermal diffusion is much higher than oxygen diffusion. Thus, a larger region might be afforded partial metabolic protection, even if oxygen cannot be delivered.

It should also be noted that perfusion cooling in the vicinity of an ischemic area would enhance ischemic region cooling, so long as the blood perfusate is at a lower temperature than the ischemic tissue. Conversely, if the blood perfusate is at a higher temperature than the conduction-cooled tissue, such as might occur in the vicinity of a near-surface ischemic region, the surface cooling effect would be blunted by the warm blood perfusate.

Head Cooling With a Convection Cooled Helmet. In this sequence of FEM simulations of brain cooling, a realistic 3-D human head was assumed covered by a cooling helmet [1]. The helmet has been simulated with convection boundary conditions on the regions where the helmet would contact the head. The face, eyes and nose were assumed uncovered and maintained at room temperature of 25°C.

The following three test cases were analyzed:

Case 5. No tissue perfusion and surface heat transfer coefficient $h_{surf}=25.0\ W\,m^{-2}\,°C^{-1}$ (derived from [1]).

Case 6. Tissue perfusion with $\theta_{art}=37°C$ at all internal elements of the head. The perfusion distribution was identical to this of Case 2.

Case 7. All other conditions were the same as in Case 6, but $h_{surf}=46.0\ W\,m^{-2}\,°C^{-1}$ (the highest value observed in [1]).

Case 5. Surface Convection Cooling Via Helmet Applied at t=0, With a Circulating Cooling Fluid at 5.5°C. No Tissue Perfusion. Temperature profiles predicted at six points within the brain (Fig. 2) are given in Fig. 12. At 30 min the outer cortical positions (C,D,E) have cooled below 35°C. However, the inner cortical regions are only beginning to cool. The heat extracted from the head (input power) calculated for that portion covered by the cooled garment is shown in Fig. 12. The total heat extraction over 60 min is 150 kJ.

Case 6. The Surface Convection Conditions of Case 5, With $\theta_{art}=37°C$ Tissue Perfusion. The temperature evolution profiles predicted at the six sites in the brain are shown in Fig. 13. There is negligible cooling (less than 0.1°C) at all sites at 30 min. Brain cooling is less efficient when a helmet is interposed between the scalp and the cold source. This is more evident when the cooling fluid is at 5.5°C rather than the ice temperature of Case 2, and even more evident when no pre-cooling of the cerebral arterial blood is assumed, also as in Case 2. These results emphasize the conclusions of Cases 1–4, that cooling of cerebral arterial blood (performed extracranially) is necessary.

Case 7. The Surface Convection Coefficient is Increased to 46 $W\,m^{-2}\,°C^{-1}$, the Highest Value Extracted From the Cited Experimental Study [1]. Other Conditions as in Case 6. Almost doubling the convective heat transfer coefficient of Case 6 provides negligible cooling of the brain (Fig. 14).

IV. Numerical Results for Neck Cooling

Due to the need to cool the blood perfusing the brain, it was decided to numerically simulate independent means of cooling of the neck. The objective was to learn if neck-only cooling would be sufficient to reduce the arterial blood temperature before it enters the brain. The neck-only geometric model was created where cylindrical neck, cervical vertebral, tracheal and carotid arterial and jugular venous dimensions were estimated from the

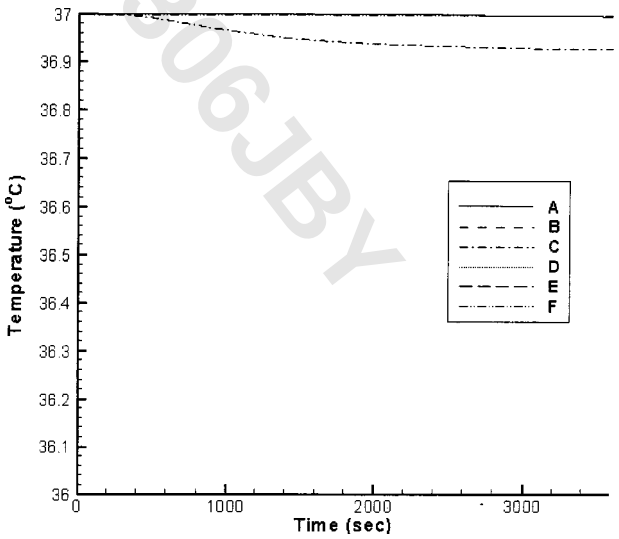

Fig. 13 Temperature evolution at monitor points in the brain for Case 6 with cooled helmet (tissue perfusion with $\theta_{surf}=0°C$, $h_{surf}=25.0\ W\,m^{-2}\,°C^{-1}$ and $\theta_{art}=37°C$ at all internal elements of the head)

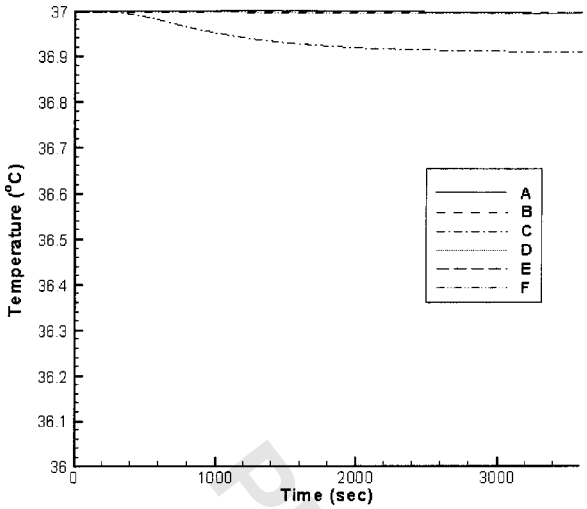

Fig. 14 Temperature evolution at monitor points in the brain for Case 7 with cooled helmet (tissue perfusion with $\theta_{surf}=0°C$, $h_{surf}=46.0\,W\,m^{-2}\,°C^{-1}$ and $\theta_{art}=37°C$ at all internal elements of the head)

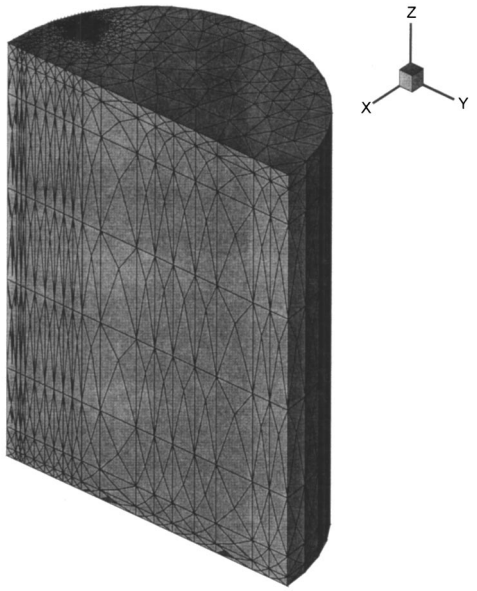

Fig. 16 Material regions and geometry for the idealized neck model

www.vesalius.com website data. Due to symmetry, only half the neck was modeled (Fig. 15) with different tissue regions shown in Fig. 16.

In the neck model, the chest (bottom) portion of the neck was set to 37°C except at the vein outlet. The top of the neck model used an insulating thermal boundary condition except for the vein inlet and artery outlet. With this boundary condition, the head and neck models can be uncoupled, which significantly reduces the computational cost. Use of this boundary condition implies the temperature in the bottom of the head and the top of the neck is the same, which is a conservative assumption.

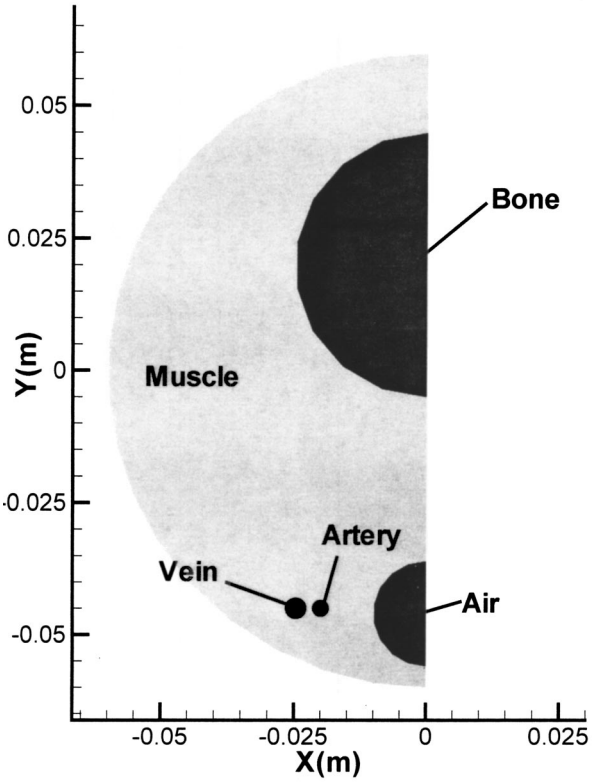

Fig. 15 Triangular surface mesh for neck model

Carotid arterial entry temperature was $\theta_{art}=37°C$. Jugular vein entry temperature was arbitrarily set at 33°C, to simulate target temperature cooling of the brain achieved from other sources (helmet, pharynx, axilla, etc.). For all cases that were analyzed, a steady, fully developed blood flow was assumed in both the artery and the vein. A zero normal heat flux was set at both the vein and artery outlet. The peak arterial blood velocity was varied from high-normal ($V_{max}=0.5\,m\,s^{-1}$) to very low ($V_{max}=0.05\,m\,s^{-1}$) as might be assumed in case of a severe stroke. The time averaged high-normal peak velocity was estimated from plotted vector Doppler-ultrasound measurements found on the www.nwra.com website.

The following case was simulated numerically.

Case 8. No tissue perfusion was assumed and $\theta_{surf}=0°C$ was applied at the neck surface thus simulating countercurrent heat exchange between jugular vein and carotid artery. Various values of peak arterial blood velocity were used.

Case 8. Steady-State Ice Cooling of the Neck With Countercurrent Heat Exchange Between Jugular Vein and Carotid Artery. In this case, a steady state simulation of the neck cooling was performed. The perfusion in the neck tissue was neglected since the perfusion constant is relatively small. This represents a best possible case and was used to determine the lowest possible arterial blood outlet temperature achievable with various carotid blood peak velocities. Figure 17 depicts the steady state temperature distributions for $V_{max}=0.5\,m\,s^{-1}$ on a slice through the neck that goes through both artery and vein. The cooling front does not reach the artery in these views. It is blocked by the countercurrent heat exchange from the warmer 33°C down-coming venous blood. At the elevation of the base of the skull (14 cm) the centerline carotid arterial blood has still not begun to cool below 37°C. However, the bulk average blood temperature shows a modest impact of neck cooling, despite the blocking thermal effect of the countercurrent exchange. The average computed temperature in the artery for various locations in the neck is shown in Table 2.

However, it is important to note that tissue perfusion at arterial temperature, which would warm the blood, was not included in

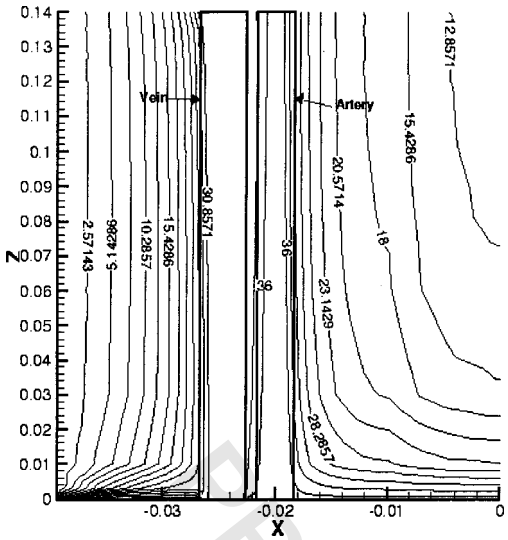

Fig. 17 Steady-state isotherms on neck slice that passes through both vein and artery (V_{max}=0.5 m/s) for Case 8 (no tissue perfusion and θ_{surf}=0°C)

this simulation. Figure 18 depicts the steady state artery outlet temperature profile for various values of peak blood velocity in the artery. The average outlet temperatures for the profiles in Fig. 18 are listed in Table 3.

For normal carotid blood flow rates, even in the steady state, the artery outlet temperature cannot be significantly reduced from

Table 2 Average blood temperature in the neck artery at different locations

Distance From Neck Base (cm)	Average Temperature (°C)
2.0	36.6
6.0	36.0
10.0	35.6
14.0	35.5

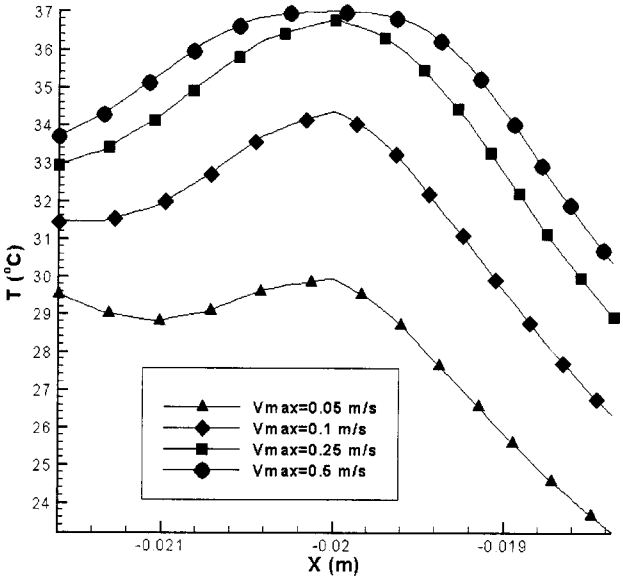

Fig. 18 Artery outlet temperature profile along the artery diameter in the x-direction for various values of peak blood velocity for Case 8 (no tissue perfusion and θ_{surf}=0°C)

Table 3 Average outlet blood temperature in the neck artery for different peak blood velocity

Peak Velocity (m/s)	Average Outlet Temperature (°C)
0.50	35.3
0.25	34.3
0.10	31.7
0.05	28.0

37°C. However, the simulations show that the blood in the artery can be cooled significantly if the blood velocity is reduced by an order of magnitude from its normal value.

It should be pointed out that the time averaged peak speed for the carotid blood is around V=0.5 m/s. It is likely even higher than that considering the range of mass flow rates quoted in the literature. For the case of peak blood speed V=0.5 m/s, the computed results show only slight cooling of the blood at the artery outlet. This agrees with theoretical and experimental data since a peak blood speed V=0.5 m/s is most often used. The purpose of using different peak average blood speeds in the simulations was to show what could be achieved if the blood flow rate would be reduced.

V. Discussion

The perfusion term in the Pennes equation is $M_b C_p(\theta_{art}-\theta)$ where M_b is the capillary perfusion rate, measured in ml blood flow per minute per ml of tissue. This "rate" can be understood as blood flow through the millions of capillaries in the tissue, proceeding in all directions at once, and thus not having a vector form. Furthermore, the extremely small capillary diameters and the relatively low blood velocity in the capillaries ensure that the blood temperature equilibrates with that of the immediately surrounding tissue before the blood leaves the capillaries. The magnitude of this perfusion heat flow term is, in general, much larger than the conduction heat flow term for temperature gradients achievable in human thermal physiology. Comparison of conduction-only versus perfusion plus conduction heat exchange in an experimental animal series amply demonstrates this important point [3,4].

Therefore, only by artificially cooling the arterial blood was it possible to cool the brain in the specified time (Cases 3, 4). Even pre-cooling arterial blood to θ_{art}=35°C did not achieve 33°C global cooling of the brain within 30 min! The helmet with 5.5°C coolant did no better when the protective effect of warm perfusion was included; the core of the brain was not cooled within 30 min for any condition (Cases 6 and 7). Ice bath cooling of the neck, provided a small measure of carotid arterial precooling of the brain resulting in θ_{art}=35.5°C average arterial temperature at 30 min. However, the model did not include tissue perfusion with warm blood, which would have substantially reduced the cooling effect.

All of this suggests that other cooling means should be explored, including: 1) combinations of currently considered external cooling methods; 2) other external methods not yet addressed; 3) internal cooling methods [20].

There are other appealing external cooling methods. Ice conditions can be applied to the axillae, and groin, regions with good coupling to arterial and venous supplies. The turbinate sinuses and pharynx, proximal to the undersurface of the frontal brain, can be convectively cooled with sublimating oxygen crystals.

Finally, there are invasive methods, including swallowing of cold fluids, and blood access technologies which might be considered. These are less desirable because of technical considerations, the advanced degree of knowledge and training that would be required, and the danger of embolization of the carotid arterial plaque burden frequently observed in stroke patients. As shown in successful clinical trials, the cooling effect of 4°C saline (1 to 2

liters) injected in the main artery would be much larger and more immediate [20] than that of any test case studied in this paper. However, this cooling effect would be transient, not continuous, and it would require an invasive procedure.

VI. Conclusions

The simulations of cooling methods considered to date all indicate that no single means of external cooling of the head or neck is sufficient to reach the 33°C target temperature in a reasonable period of time. Specifically, for the iced surface of the head, inclusion of the warm blood perfusion term effectively blocks the cooling wave from advancing beyond a few millimeters at 30 min.

The central conclusion of insufficient cooling is supported by the modest cooling enhancements reported in other experimental investigations of externally applied cooling [1,2,19]. While experiments might be conducted with optimized cooling conditions, such as shaving the head, applying closer-fitting head and neck garments, convective enhancement of the head or neck ice baths, none of these means are likely to change the conclusion in conservative application of the method.

In simulations for head subjected to both constant surface temperature and convection, the face, eyes, and nose were assumed to be at the steady room temperature which might not be realistic considering the 3-D heat transfer. It should not be too difficult to incorporate a natural convection boundary condition on these surfaces in the model. However, since the results are dominated by the effect of the blood perfusion and not the surface boundary conditions in these small areas, changing these boundary conditions would not change the overall results significantly.

Acknowledgments

The authors are grateful to Dr.-Ing. Frank B. Sachse, Institute of Biomedical Engineering, University of Karlsruhe for providing a digitized geometry of a real human head.

Nomenclature

C_p = Coefficient of specific heat
h_{surf} = Surface thermal convection coefficient
K = Thermal conduction coefficient
M_b = Capillary perfusion rate
Q = Surface heat flux
q_m = Metabolic heat source
T = Time
V = Peak blood speed
x,y,z = Cartesian coordinates
ρ = Density of the living tissue
θ = Temperature
θ_{art} = Artery blood temperature
θ_{surf} = Surface temperature

References

[1] Ku, Y.-T., Montgomery, L. D., and Webbon, B. W., 1996, "Hemodynamic and Thermal Responses to Head and Neck Cooling in Men and Women," Am. J. Phys. Med. Rehabil., **75**(6), pp. 443–450.
[2] Orr, C. S., and Eberhart, R. C., 1998, "Bioheat Transfer in Blood Perfused Tissues and Clinical Application of Hypothermia," Chapter 1 in *Annual Review of Heat Transfer*, ed.: C. L. Tien, Begell House, New York, pp. 1–78.
[3] Olsen, R. W., 1985, "Temperature Profiles in the Head and Other Tissues of the Macaque Rhesus Monkey Subjected to Surface and/or Core Cooling," Ph.D. Dissertation, University of Texas Southwestern Medical Center at Dallas, Dallas, Texas.
[4] Olsen, R. W., Hayes, L. J., Wisler, E. H., Nikaidoh, H., and Eberhart, R. C., 1985, "Influence of Hypothermia and Circulatory Arrest on Cerebral Temperature Distributions," ASME J. Biomech. Eng., **107**, pp. 354–360.
[5] Vietla, S., 1995, "The Influence of Hypothermia and Tissue Perfusion on Temperature Distribution in Simulated Intracranial Surgery," M.Sc. thesis, University of Texas Southwestern Medical Center at Dallas, Dallas, TX.
[6] Pennes, H. H., 1948, "Analysis of Tissue and Arterial Blood Temperatures in the Resting Forearm," J. Appl. Physiol., **1**, pp. 93–122.
[7] Huebner, K. H., Thorton, E. A., and Byrom, T. G., 1995, *The Finite Element Method for Engineers*, John Wiley and Sons, New York, NY, 3rd edition.
[8] Balay, S., Gropp, W. D., McInnes, L. S., and Smith, B. F., 1999, "PETSc 2.0 Users Manual," Technical Report ANL-95/11—Revision 2.0.24, Argonne National Laboratory.
[9] Dennis, B. H., and Dulikravich, G. S., 1999, "Simultaneous Determination of Temperatures, Heat Fluxes, Deformations, and Tractions on Inaccessible Boundaries," ASME J. Heat Transfer, **121**, pp. 537–545.
[10] Dennis, B. H., and Dulikravich, G. S., 2000, "Determination of Unsteady Container Temperatures During Freezing of Three-Dimensional Organs With Constrained Thermal Stresses," In: *Internat. Symposium on Inverse Problems in Engineering Mechanics—ISIP'2k*, eds: M. Tanaka and G. S. Dulikravich, Nagano, Japan, March 7–10, 2000, Elsevier Science Ltd, Amsterdam, pp. 139–148.
[11] Dennis, B. H., Dulikravich, G. S., and Rabin, Y., 2000, "Optimization of Organ Freezing Protocols With Specified Allowable Thermal Stress Levels," ASME IMECE 2000, Orlando, FL, Nov. 5–10, 2000, HTD-Vol. 368/BED-Vol. 47, pp. 33–48.
[12] Proceedings of First Users Conference of the National Library of Medicine's *Visible Human Project*, October 7–8, 1996, National Institute of Health, Bethesda, MD.
[13] Sachse, F., Werner, C., Müller, M., and Meyer-Waarden, K., 1996, "Preprocessing of the Visible Man Dataset for the Generation of Macroscopic Anatomical Models," Proc. First Users Conference of the National Library of Medicine's *Visible Human Project*, October 7–8, 1996, National Institute of Health, Bethesda, MD.
[14] Sachse, F., Werner, C., Müller, M., and Meyer-Waarden, K., 1996, "Segmentation and Tissue-Classification of the Visible Man Dataset Using the Computertomographic Scans and the Thin-Section Photos," Proc. First Users Conference of the National Library of Medicine's *Visible Human Project*, October 7–8, 1996, National Institute of Health, Bethesda, MD.
[15] Shitzer, A., and Eberhart, R. C. (eds.), 1985, *Heat Transfer in Medicine and Biology: Analysis and Applications*, *Volume II*, Appendix II, Plenum Press, New York.
[16] Shitzer, A., and Eberhart, R. C. (eds.), 1985, *Heat Transfer in Medicine and Biology, Analysis and Applications*, *Volume 1*, Plenum Press, New York, Chap. 12, pp. 279–283.
[17] Bowman, H. F., Cravalho, E. G., and Woods, M., 1975, "Theory, Measurement, and Application of Thermal Properties of Biomaterials," Annu. Rev. Biophys. Bioeng., **4**, pp. 43–80.
[18] Valvano, J. W., Cochran, J. R., and Diller, K. R., 1985, "Thermal Conductivity and Diffusivity of Biomaterials Measured With Self-Heated Thermistors," International Journal of Thermophysics, **6**(3), pp. 301–310.
[19] Corbett, R. J. T., and Laptook, A., 1988, "Failure of Localized Head Cooling to Reduce Brain Temperature in Adult Humans," NeuroReport, **9**, pp. 2721–2725.
[20] Bernard, S. A., Jones, B. M., and Horne, M. K., 1997, "A Clinical Trial of Induced Hypothermia in Comatose Survivors of Prehospital Cardiac Arrest," Ann. Emerg. Med., **30**, pp. 146–153.